Contrib Mineral Petrol (2007) 154:439–453
DOI 10.1007/s00410-007-0202-z

ORIGINAL PAPER

Insights from quartz cathodoluminescence zoning into crystallization of the Vinalhaven granite, coastal Maine

R. A. Wiebe · D. A. Wark · D. P. Hawkins

Received: 21 November 2006 / Accepted: 3 April 2007 / Published online: 26 April 2007

Abstract The Vinalhaven intrusive complex provides field and petrographic evidence for multiple replenishments of mafic and silicic magmas, mingling and limited mixing, and rejuvenation of granite. Quartz in granitic rocks preserves a record of those processes, in the form of cathodoluminescence (CL) zoning, which is related to concentration of titanium, and to temperature of crystallization using the new TitaniQ (Ti in quartz) geothermometer. Injection of mafic melts into partly crystalline Vinalhaven granite resulted in partial quartz resorption followed by higher-temperature growth from H_2O-undersaturated melt. This is shown by steep, rimward increases in CL intensity and Ti content across discordant boundaries that truncate older growth zones. Quartz zoning in granite affected by mafic magmas displays large rimward jumps in Ti content, whereas quartz in granitic feeders and in granite far from mafic rocks typically displays broad rims with decreasing Ti contents, consistent with slow cooling without thermal disruptions due to mafic recharge.

Communicated by T.L. Grove.

R. A. Wiebe (✉)
Department of Earth and Environment,
Franklin and Marshall College,
Lancaster, PA 17603, USA
e-mail: bwiebe@fandm.edu

D. A. Wark
Department of Earth and Environmental Sciences,
Rensselaer Polytechnic Institute, Troy,
NY 12180, USA

D. P. Hawkins
Department of Geosciences, Denison University,
Granville, OH 43023, USA

Introduction

Compositional zoning in minerals provides the clearest record of the crystallization history and conditions of plutonic igneous rocks. In particular, compositional zoning in plagioclase (e.g., Wiebe 1968; Loomis and Welber 1982; Wallace and Bergantz 2005) and accessory minerals (Robinson and Miller 1999) has long been recognized as an important source of information about magma chamber processes. Recently, several studies have shown that quartz in plutonic rocks can also preserve delicate cathodoluminescence (CL) zoning that could provide comparable information about crystallization history (D'Lemos et al. 1997; Müller et al. 2000, 2005). The potential value of quartz zoning has been greatly enhanced by the recent recognition that CL intensity is related to the concentration of Ti in quartz (Wark and Spear 2005) and the recent development of a Ti in quartz thermometer (Wark and Watson 2006).

CL zoning in quartz has the potential to contribute a wealth of information about the crystallization history and magmatic processes that produce granite. To test this potential, we undertook a systematic study of all felsic rocks in the Vinalhaven intrusive complex (Wiebe et al. 2004). Because intensive field, petrographic and geochemical studies have been carried out on the Vinalhaven granitic rocks and many aspects of their crystallization appear to be well constrained, these rocks provide an opportunity to test to what extent quartz crystallization either reflects these processes or requires new interpretations of crystallization history. The Vinalhaven intrusive complex preserves evidence for a wide range of magmatic processes, including crystallization, episodic replenishment, mingling of mafic and felsic magmas and rejuvenation of granite. Because all felsic magmas in this complex were saturated in quartz at

emplacement, quartz zoning should record all stages of crystallization. The goal of this paper is to document the extent to which quartz zoning reflects magmatic processes inferred from detailed field, petrographic and geochemical studies and to what extent it conflicts with or adds new insights to those studies. The results presented below indicate that quartz zoning provides a clear record of processes inferred from field relations and suggest that quartz zoning may prove even more valuable in studies of granitic bodies that lack robust field constraints.

The Vinalhaven intrusive complex

Regional geologic setting

The Vinalhaven intrusive complex is located on Vinalhaven Island in southern Penobscot Bay, about 15 km east of Rockland, Maine (Fig. 1). The complex belongs to the Coastal Maine Magmatic Province, an association of more than 100 granitic and mafic plutons that intruded parallel to NE trending fault-bounded terranes from the Late Silurian to Early Carboniferous (Hogan and Sinha 1989). The terranes consist primarily of pre-Devonian metavolcanic and metasedimentary rocks and are thought to be microplates of continental crust that accreted onto the North American craton during the Acadian Orogeny (Hogan and Sinha 1989). Hogan and Sinha (1989) proposed that post-accretion magmatism in the Coastal Maine Magmatic province is related to rifting in a trans-tensional environment where crustal extension and lithospheric thinning allowed for the emplacement of mafic magma at various crustal levels. A subsequent shift to a trans-pressional regime is thought to have trapped mafic magma at the base of the crust and induced partial melting of the overlying granitic crust. Gravity studies suggest that most granitic plutons are only a few km thick, and lie above mafic rocks (Hodge et al. 1982).

In the ~420 Ma Vinalhaven intrusive complex, magmatism is strongly bimodal with widespread interactions of coeval mafic and silicic magmas. Basaltic rocks are low-K tholeiites with trace element characteristics comparable to back arc basalts and with ε_{Nd} ~ +6 to +7 and Sr_i ~ 0.702 to

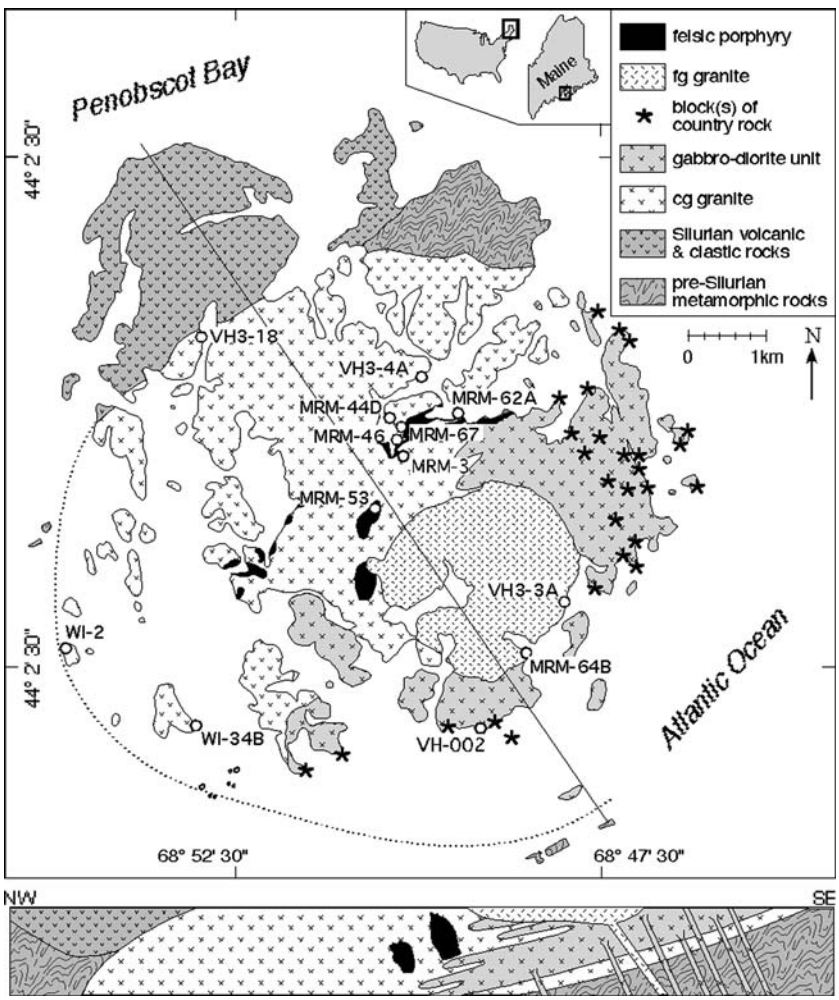

Fig. 1 Geologic map of the Vinalhaven intrusive complex

3 (Hawkins, unpublished data). Granitic rocks approach low pressure mininum melt compositions; their isotopic compositions, ε_{Nd} ~ –1 to –2; Sr_i ~ 0.706 to 7, are highly contrasted with the basalts (Hawkins, unpublished data).

Field relations

The Vinalhaven intrusive complex, roughly 12 km in diameter, consists of three main units, coarse-grained (cg) granite, gabbro-diorite and fine-grained (fg) granite, and several smaller bodies of felsic porphyry (Wiebe et al. 2004) (Fig. 1). It was constructed over about 1 m.y. by replenishments of both granitic and basaltic magmas (Hawkins, unpublished U–Pb ages). It intrudes deformed, low-grade early Paleozoic schists and, along its northwestern margin, weakly deformed coeval volcanic rocks that include rhyolite flows and tuffs. Cg granite underlies most of the island and has a well-exposed contact with country rock along its northern (upper) margin (Fig. 1). In the southeastern half of the complex, cg granite is underlain by the gabbro-diorite unit, which consists of interlayered mafic, hybrid, and granitic rocks. This unit forms a curved, sheet-like body, 100's of meters to more than 1 km thick, which dips 10–30° to the north and west beneath the granite. Extensive blocks of country rock, identical to country rock in the northern part of the island, occur within the gabbro-diorite unit (Hawkins and Wiebe 2004). Metamorphism of pelitic blocks suggests pressures of approximately 1 kb (Porter et al. 1999).

A body of fg granite cuts through the gabbro-diorite unit and forms a core of the complex, about 3–4 km in diameter (Fig. 1). Contacts with cg granite are sharp in the south, but locally gradational and commingled in the north. Dikes of similar fg granite up to 25 m thick cut through the gabbro-diorite unit and appear to be feeders for silicic replenishments to the complex (Wiebe and Hawkins 2004).

Most of the gabbro-diorite can be subdivided into macro-rhythmic units (layers), each of which is marked by a chilled gabbroic base. These units vary in thickness from less than one to more than 100 m. Where they are more than 10–20 m thick, they commonly grade upward to hybrid dioritic and granitic rocks that display evidence for incomplete mixing between mafic and felsic magmas. Widespread load-cast and pipe structures at the chilled mafic bases of macrorhythmic units indicate the gabbro-diorite unit formed by a sequence of basaltic injections that ponded at the base of an aggrading silicic magma chamber and variably interacted with overlying granitic magma (Wiebe 1993; Wiebe and Collins 1998).

Cg granite is massive and leucocratic. Gently dipping groups of planar to cross-bedded and arcuate schlieren occur locally in the granite as thin (<1 cm) layers enriched in mafic minerals. They closely resemble similar features that have been widely reported in other granites (e.g., Gilbert 1906; Emeleus 1963). Their attitudes are generally consistent with the framework established by the inward dipping (basin-form) mafic layers and the western margin of the pluton. Granite contains scarce felsic porphyry enclaves typically between 20 cm and 1 m in diameter and larger blocks of texturally variable, more leucocratic granite. Small (<1 cm) granular mafic enclaves occur sparsely in many areas of the granite; their source appears to be the basaltic input that generated the mafic sheets within the granite. Their wide distribution suggests that cg granite crystallized from magma that was convectively stirred (Wiebe and Hawkins 2004).

Bodies of porphyry (Fig. 1) have contacts with cg granite that vary from sharp and planar (cutting crystals) to gradational over several cm and highly convoluted (exchange of crystals). They typically contain scarce cm-scale quenched mafic enclaves. The largest body of porphyry (Fig. 1) was produced when a 60 meter-thick basaltic dike was emplaced into and remobilized nearly solid granite (Wiebe et al. 2004). At one contact, a ~20 cm thick zone of strongly quenched porphyry separates cg granite from chilled gabbro. Porphyry in the southern (basal) part of this body is phenocryst-rich with a strongly quenched matrix; toward the northern (upper) contact the porphyry decreases in phenocryst abundance and increases in matrix grain size (Wiebe et al. 2004). The compositional and petrographic similarity between this porphyry and other smaller bodies of porphyry (including the felsic enclaves) suggest that all porphyry represents granitic magma that was rejuvenated due to input of mafic magma.

Petrography

Cg Vinalhaven granite has a color index between 7 and 2 and is dominated by subhedral, weakly tabular, pink, perthitic alkali-feldspar (3–10 mm in length) with subordinate smaller, blocky white plagioclase and equant quartz (3–6 mm). Alkali feldspar shows coarse perthitic exsolution and, uncommonly, faint subhedral zoning. Plagioclase has delicate, oscillatory–normal zoning, mainly $An_{27–20}$. Equant quartz crystals commonly occur clustered together between the large alkali feldspars. Mafic minerals consist mainly of biotite, locally with minor hornblende, and accessory Fe–Ti oxides (ilmenite and magnetite), allanite, apatite, and zircon. All of these minerals occur as inclusions in quartz and both feldspars; Fe–Ti oxides occur in some crystallized melt inclusions in quartz. Subhedral Fe–Ti oxides are commonly included in biotite and hornblende. Sphene occurs sparsely on the margins of mafic clots and appears to be a subsolidus reaction product. Scarce small mafic enclaves are very fine-grained and dominated by roughly equal amounts of blocky to tabular

plagioclase and hornblende, with a few percent Fe–Ti oxides and biotite.

Several small bodies of porphyry and the porphyry enclaves in cg granite have between 5 and 45% phenocrysts that are similar in identity, size and composition to minerals in cg granite (Wiebe et al. 2004). Most phenocrysts are anhedral and appear to be highly corroded, and many have reaction rims. Adjacent crystals may vary greatly in their degree of corrosion and reaction. Alkali feldspar phenocrysts may be anhedral and lack plagioclase overgrowths or have plagioclase rims that vary in thickness from a few microns to about 1 mm. Plagioclase phenocrysts have compositions and zoning similar to that in the granite, although plagioclase phenocrysts and plagioclase rims on K-feldspar commonly contain many patches of microgranophyric intergrowths of quartz and K-feldspar (Wiebe et al. 2004). The anhedral margins of plagioclase commonly truncate delicate oscillatory zoning, as do fretted rims (up to 300 μm thick) with minute quartz and alkali-feldspar inclusions. Some quartz phenocrysts have prominent hornblende ± biotite reaction rims, whereas other nearby phenocrysts may lack rims. Biotite and scarce allanite phenocrysts are typically anhedral and commonly have poikilitic overgrowths that extend into the very fine-grained matrix. The grain size and textures of the porphyry matrix vary widely. The finest-grained matrix is aphanitic with acicular apatite and is dominated by microgranophyric intergrowths of quartz and alkali-feldspar along with plagioclase and biotite (mostly 10–100 μm in diameter). More commonly, the matrix has coarser granophyric textures along with plagioclase crystals that are subequant and range from 50 to 300 μm in diameter. Microgranophyric textures also occur commonly as overgrowths on quartz.

Fg granite has major and accessory minerals identical to those in the cg granite. Grain-sizes are typically in the ranges: K-feldspar (0.5–4 mm), plagioclase (0.5–2 mm), quartz (0.3–1 mm), and biotite (<1 mm). Somewhat finer and coarser varieties are locally commingled in the fg granite body, and dikes are on average finer grained than the larger equant body.

Mafic rocks that crystallize away from granite have largely an anhydrous mafic mineralogy dominated by augite and olivine. Where they mingle with granitic magmas, the resulting quenched basaltic pillows typically have abundant hornblende and biotite and may lack augite and olivine.

Analytical methods

Whole-rock samples were analyzed for major and trace elements by X-ray fluorescence (XRF) at Franklin and Marshall College using a Philips 2404 XRF vacuum spectrometer equipped with a 4 kW Rh X-ray tube. For major element analysis nine parts $Li_2B_4O_7$ was mixed with one part rock powder and fused into a homogeneous glass disk. Working curves were determined by analyzing 51 geochemical rock standards, data for each having been compiled by Govindaraju (1994). Analytical errors associated with measuring major element concentrations range from <1% for Si and Al to 3% for Na. Trace element briquettes were prepared by mixing 7 g of whole rock powder with 1.4 g of pure microcrystalline cellulose. Analytical errors for the trace elements range from 1 to 2% for Rb, Sr, Y, Zr, etc., to 5 to 6% for Ba.

Cathodoluminescence images of quartz were collected from carbon-coated polished sections using the miniCL system purchased from Oxford Instruments (now Gatan, Inc.), which is attached to the JEOL733 Superprobe at Rensselaer. Most images were gathered using an accelerating voltage of 15 kV, a beam current between 15 and 20 nA, and a dwell time of 0.5–1 s per pixel.

Analyses of Ti concentrations in quartz were performed using the Cameca SX100 electron microprobe at Rensselaer. To minimize analytical uncertainties, counts were collected simultaneously on three spectrometers—each equipped with a large-area PET crystal and averaged. Although analyses were performed at 15 kV accelerating voltage, a current of 200 nA, and a spot size of 10–20 μm, the calibration of Ti count rates was performed on a synthetic rutile standard with a focused beam at a current of only 10–20 nA (also at 15 kV) to minimize pulse-height analyzer peak shifts at high count rates. With count times of 240 s per spot, analytical uncertainties (1 sigma) are on the order of 10 ppm Ti.

Geochemistry

All varieties of granitic rocks and porphyry have between 72.5 and 77.5 wt.% SiO_2, consistent with early crystallization of quartz (Table 1; Fig. 2). The dominant cg and fg granites and porphyry range from about 73 to 77 wt.% silica. Felsic enclaves, which show some evidence of contamination by mafic magma, extend to as low as 70 wt% SiO_2 (Fig. 2). Fine-grained felsic dikes (not shown) vary from about 75 to 78 wt.%. With the exception of K_2O, which increases with SiO_2, major element concentrations of all granitic rocks decrease as SiO_2 increases and define relatively tight trends (Fig. 2). All of these rocks have compositions that lie close to the 1 kb minimum in the system SiO_2-ab-or-H_2O (Fig. 3). Trace elements show considerable scatter on Harker diagrams, though Nb, Sr, Ba, REE's and Y broadly decrease and Rb, Th and U increase as SiO_2 increases. Well defined decreasing trends of Zr, V, P_2O_5, TiO_2, and FeO_t vs increasing SiO_2 lend support to textural evidence which suggests biotite, Fe–Ti oxides, zircon and apatite were on the liquidus throughout the crystallization of this ~mini-

Table 1 Whole rock chemical analyses of Vinalhaven granitic rocks for which quartz CL and Ti zoning are reported

Sample	MRM-64B fg granite	VH3-3A fg granite	VH3-18 cg granite	VH3-4A cg granite	MRM-62A cg granite	MRM-3 cg granite	VH-002 cg granite	WI-2 cg granite	MRM-67 Porphyry	MRM-46 Porphyry	MRM-53 Porphyry	WI-34B Enclave	MRM-44D enclave
SiO_2	73.48	73.98	75.68	75.12	74.06	73.62	72.62	77.13	75.11	72.92	72.17	71.93	70.32
TiO_2	0.28	0.34	0.27	0.24	0.34	0.33	0.40	0.21	0.20	0.35	0.40	0.43	0.62
Al_2O_3	13.60	14.04	12.78	13.31	13.05	13.04	13.19	12.04	13.16	13.14	13.34	13.13	13.56
Fe_2O_3	1.96	2.23	1.96	1.58	2.18	2.25	2.72	1.45	1.43	2.37	2.73	3.36	3.85
FeO	0.00	0.00	0.00	0.00	0.00	0.00	0.00	0.00	0.00	0.00	0.00	0.00	0.00
MnO	0.04	0.05	0.05	0.04	0.05	0.06	0.06	0.04	0.04	0.05	0.06	0.08	0.09
MgO	0.48	0.51	0.36	0.33	0.42	0.48	0.51	0.26	0.30	0.61	0.85	1.02	1.16
CaO	1.20	1.15	0.86	0.98	1.05	1.13	1.29	0.70	0.94	1.32	1.69	1.44	2.14
Na_2O	3.27	3.43	3.36	3.30	3.24	3.22	3.16	2.96	3.31	3.24	3.32	3.41	3.60
K_2O	5.01	5.05	4.71	5.30	5.02	5.09	4.88	4.99	5.00	4.98	4.65	4.46	4.00
P_2O_5	0.10	0.10	0.07	0.06	0.09	0.08	0.11	0.06	0.06	0.08	0.09	0.08	0.11
LOI	0.45	0.48	0.48	0.41	0.40	0.37	0.33	0.36	0.31	0.34	0.00	0.31	0.47
Total	99.86	101.37	100.57	100.66	99.89	99.67	99.27	100.20	99.85	99.39	99.30	99.65	99.93
Ba	444	480	240	312	284	311	389	208	305	303	286	99	232
Rb	195	250	225	211	197	200	177	242	252	231	201	319	184
Sr	69	62	38	48	48	49	61	32	44	53	58	30	58
Pb	22	20	24	24	20	20	21	24	27	23	22	24	21
Th	16.9	21.1	20.7	13.4	8.8	15.6	13.9	22.5	17.6	19.5	17.1	19.5	17.9
U	3.9	5.0	4.4	3.4	3.8	4.0	1.8	4.1	5.8	4.2	4.5	7.3	3.0
Zr	197	220	162	159	190	183	234	158	135	164	161	168	169
Nb	12.9	14.6	11.2	9.1	12.1	11.0	11.5	11.2	11.9	11.7	11.6	12.2	13.3
Y	41	47	43	37	37	45	31	40	34	43	49	61	57
V	25	31	25	19	34	33	36	16	13	37	44	46	74
Cr	7	7	6	2	7	15	11	5	19	17	33	31	27
Ni	3	3	2	2	3	4	4	2	1	4	9	14	9
Zn	39	35	28	23	31	38	34	26	19	29	33	47	51
Ga	17.0	17.9	16.7	16.2	16.9	17.1	17.3	14.9	16.3	17.2	16.8	17.3	18.8
Ce	66.3	94.1	50.0	41.3	76.0	91.1	61.1	77.4	59.2	35.6	102.5	45.5	68.0
La	33.7	47.3	16.0	18.5	22.2	47.6	30.5	34.7	28.3	14.7	56.6	26.7	29.7
Co	5	5	4	3	4	4	4	3	3	5	6	7	8
Sc	4	6	6	5	8	7	8	5	6	6	8	7	9

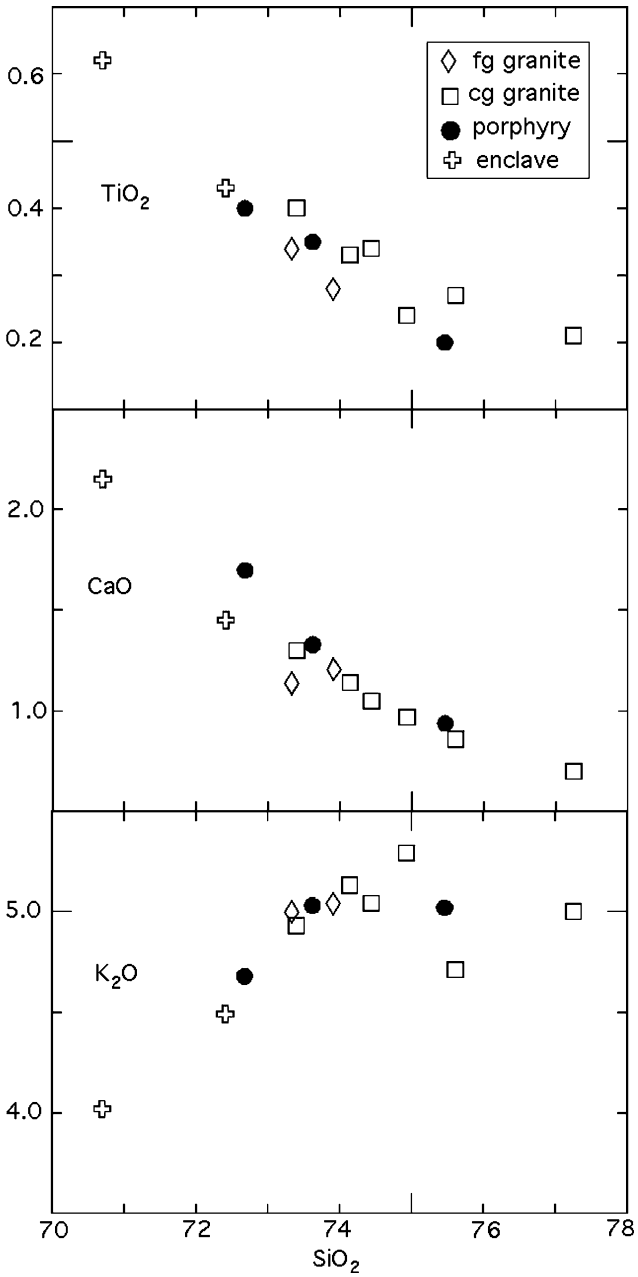

Fig. 2 Selected plots of major and trace element compositions of felsic rocks of the Vinalhaven intrusive complex

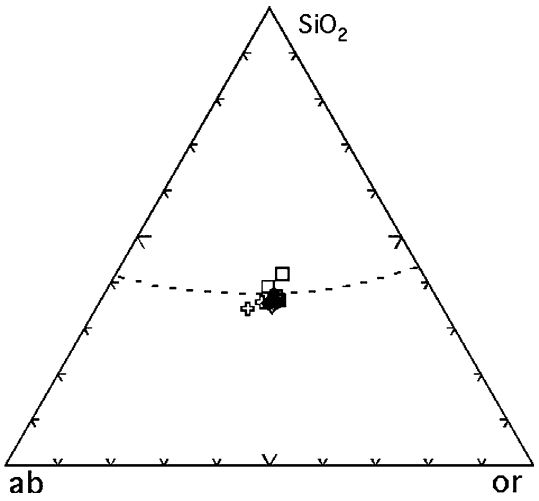

Fig. 3 Plot of granite compositions in wt.% normative SiO_2-ab-or (H_2O-saturated); minimum is for a pressure of 1 kb

mum-melt granitic magma. There is no apparent systematic spatial variation in composition throughout the cg granite, although samples from within a kilometer of the northern (upper) contact tend to have higher SiO_2.

Cathodoluminescence and Ti zoning in Vinalhaven quartz

In all Vinalhaven felsic rocks, quartz displays dominantly concentric zoning marked by variations in CL emission intensity. The zoning appears remarkably similar to the compositional zoning recognized in plagioclase crystals found in most granite. Because CL emission intensity tends to correlate with Ti concentration in igneous quartz (Wark and Spear 2005), and with temperature of crystallization (Wark and Watson 2006), we describe that zoning here. Individual zones in quartz are commonly graded in intensity—bright at an inner margin and darkening outward—consistent with declining Ti content. In the descriptions below, these zones will be termed ‘‘normal’’, in parallel with terminology for plagioclase that shows decreasing % An outward. The bright inner margins of these zones commonly enclose and sharply truncate darker inner zones. These boundaries between the inner dark zones and the bright margin are termed ‘‘reverse’’. Zoning that displays minor concentric alternations in intensity will be termed ‘‘oscillatory’’.

In most samples, irregular bands of low CL emission intensity cut primary quartz zoning. These bands appear to reflect subsolidus recrystallization in the presence of hydrothermal fluids along irregular fractures. We do not discuss these post-magmatic zones below.

Fine-grained granite and dikes

Quartz crystals in fg granitic rocks (both dikes and larger bodies) are characterized by weak, concentric CL zoning marked by small brighter cores with about 100 ppm Ti, that grade to broad darker rims characterized by normal zoning from about 70 to 40 ppm Ti (Fig. 4a). Quartz in one of three samples analyzed displays concentric zoning marked by subtle oscillations in brightness; rarely, oscillatory zones in the core appear to be truncated by thin brighter zones (Fig. 4b).

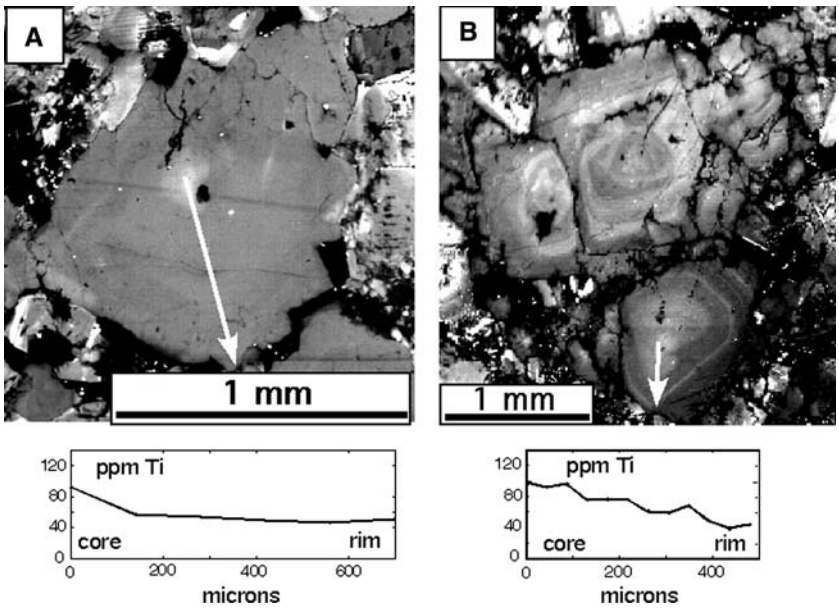

Fig. 4 Characteristic CL and Ti zoning in quartz in fine-grained granite and granitic dikes. **a** Spec. MRM-64B. **b** VH3-3A. See Fig. 1 for samples locations

Coarse-grained granite

Quartz in cg granite has more complex CL zoning and a greater range of Ti (20–140 ppm) (Fig. 5). Quartz crystals in specimens MRM-3 (Fig. 5a) and VH3-4A (Fig. 5e) are characteristic of much of the granite: zones are typically rounded and subhedral to anhedral; oscillatory normal zoning is common with individual zones having sharp brighter interior margins and darker exterior margins. Where reversals have a high contrast in brightness, inner zones are commonly truncated. Small dark rounded cores with subtle oscillatory zoning are common, and zones in these cores are commonly truncated by brighter mantles that grade outward with some oscillations to rims as dark as the cores. The rounded cores typically have between 20 and 50 ppm Ti; across the boundary separating the dark CL core from the bright mantle, Ti contents increase abruptly (from about 20 to 100 ppm in many crystals) (Fig. 5c, e). Rims are normally zoned, typically grading outward to about 40 ppm Ti (Fig. 5d, e).

Quartz crystals within a single thin-section commonly appear to have very different sequences of zones except in their outermost mantles (Fig. 5a). Comparable contrasts in zonal sequences have been noted in plagioclase zoning for many years (Wiebe 1968; Wallace and Bergantz 2005). Quartz crystals also commonly have multiple cores with concentric zoning that are truncated by a continous brighter mantle that surrounds the cores (*x* and *y* in Fig. 5a). Where the cores have different optical orientations, those orientations extend to the crystal margin, so that, in crossed polars, a multi-cored crystal with a continuous CL mantle can appear to be two or more separate, unrelated crystals. Comparable apparently synneutic relationships are well known in plagioclase feldspars (Vance 1969; Hogan 1993) and were predicted for quartz by Vance (1969).

Some areas of cg granite have quartz zoning with distinctive characteristics. In specimen MRM-62A (Fig. 5b), located near the center of the granite body within a meter of a major porphyry body, all quartz crystals have a thin bright zone either near or at the rim of the crystal. Specimen VH-002 (Fig. 5c) is from granite collected about 20 cm below the base of a chilled, 5-meter thick gabbroic sheet. All quartz crystals in this sample have mantles that are unusually bright and broad (Fig. 5c). Quartz crystals in specimen WI-2 (Fig. 5d), located near the western contact with country rock and in specimen VH3-18 (Fig. 5f), located near the uppermost contact of the granite, lack strong reversals and have unusually broad normally zoned rims. These last two areas are far from the gabbro-diorite unit (Fig. 1).

Porphyry

Although cores of quartz phenocrysts in porphyry are characterized by zoning that closely resembles quartz in cg granite, most crystals have outermost zones (rims) that are bright and truncate internal zoning (Fig. 6a–c). (These outermost rims were not analyzed in Ti profiles for Fig. 6a, c.) Quartz crystals in porphyry have ranges of Ti concentrations that are nearly identical to quartz in cg granite (Fig. 6a–d). The thin bright rims that occur on quartz in most porphyry samples typically have Ti concentrations of 120–140 ppm and represent increases of 40–60 ppm Ti over interior zones, comparable to reversals common within quartz in cg granite.

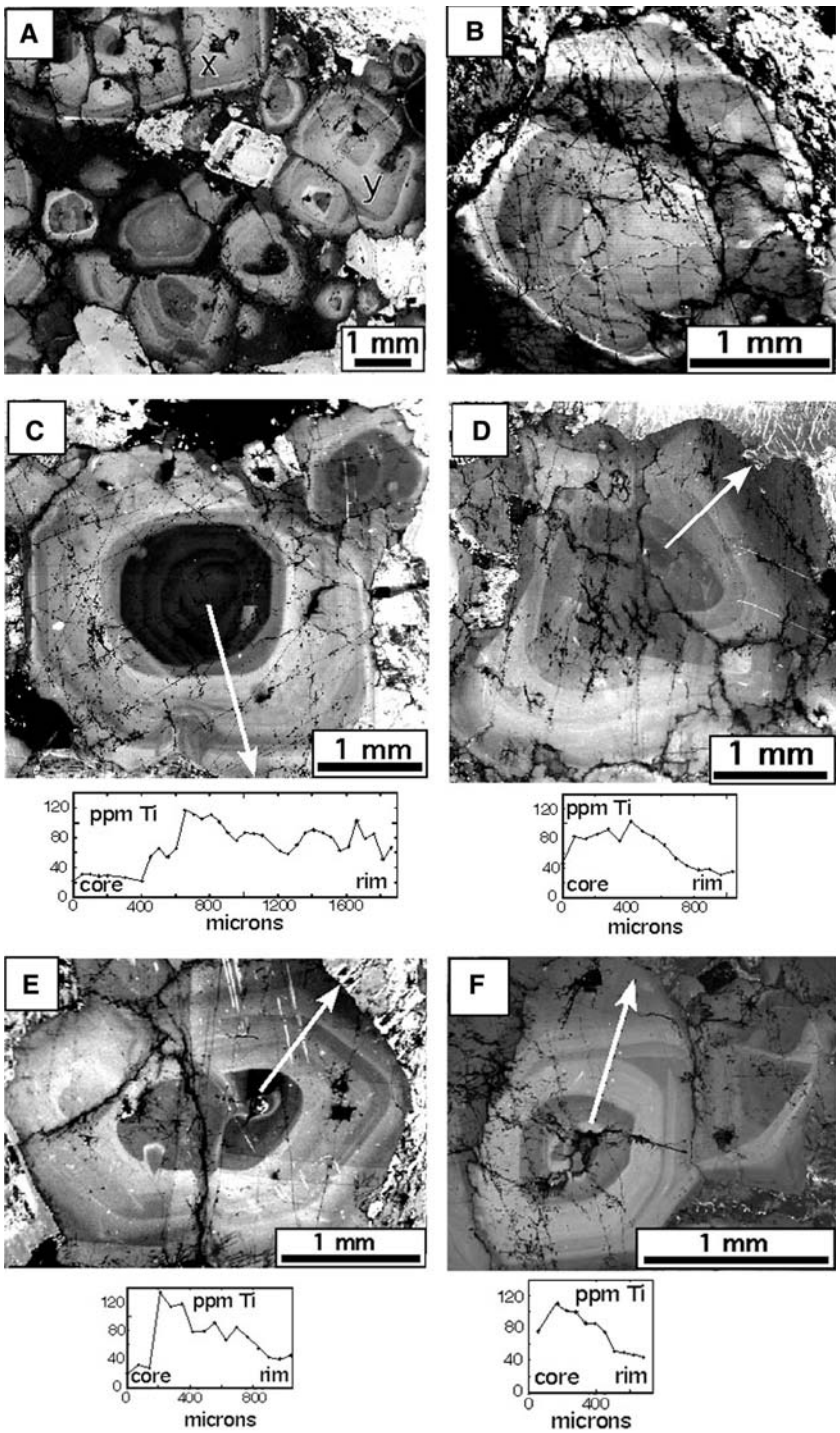

Fig. 5 Characteristic CL and Ti zoning in quartz in coarse-grained granite. **a** Spec. MRM-3. **b** Spec. MRM-62A. **c** Spec. VH-002. **d** Spec. WI-2. **e** Spec. VH3-4A. **f** VH3-18. See Fig. 1 for samples locations

Quartz phenocrysts in the southern part of the Vinal Cove porphyry (close to the large basaltic dike) have zonal sequences that are similar to that shown in Fig. 6a and occur in a strongly quenched matrix (Fig. 6b, c). Samples far from the basalt and close to the apparent roof of the Vinal Cove body have fewer phenocrysts (5–15%) and a less strongly quenched, fine-grained matrix. Quartz phenocrysts here commonly show a bright anhedral mid-zone with high Ti (~120 ppm) and broader normally zoned mantles (Fig. 6d). Other crystals have irregular bright areas within their interior and broad normally zoned mantles; some of these bright areas have shapes that strongly suggest an episode of skeletal growth (lower left in Fig. 6e).

As in quartz crystals in cg granite, apparent synneusis is common in quartz phenocrysts (Fig. 6b). In Fig. 6f an unusual rounded ‘‘phenocryst’’ consists of at least five

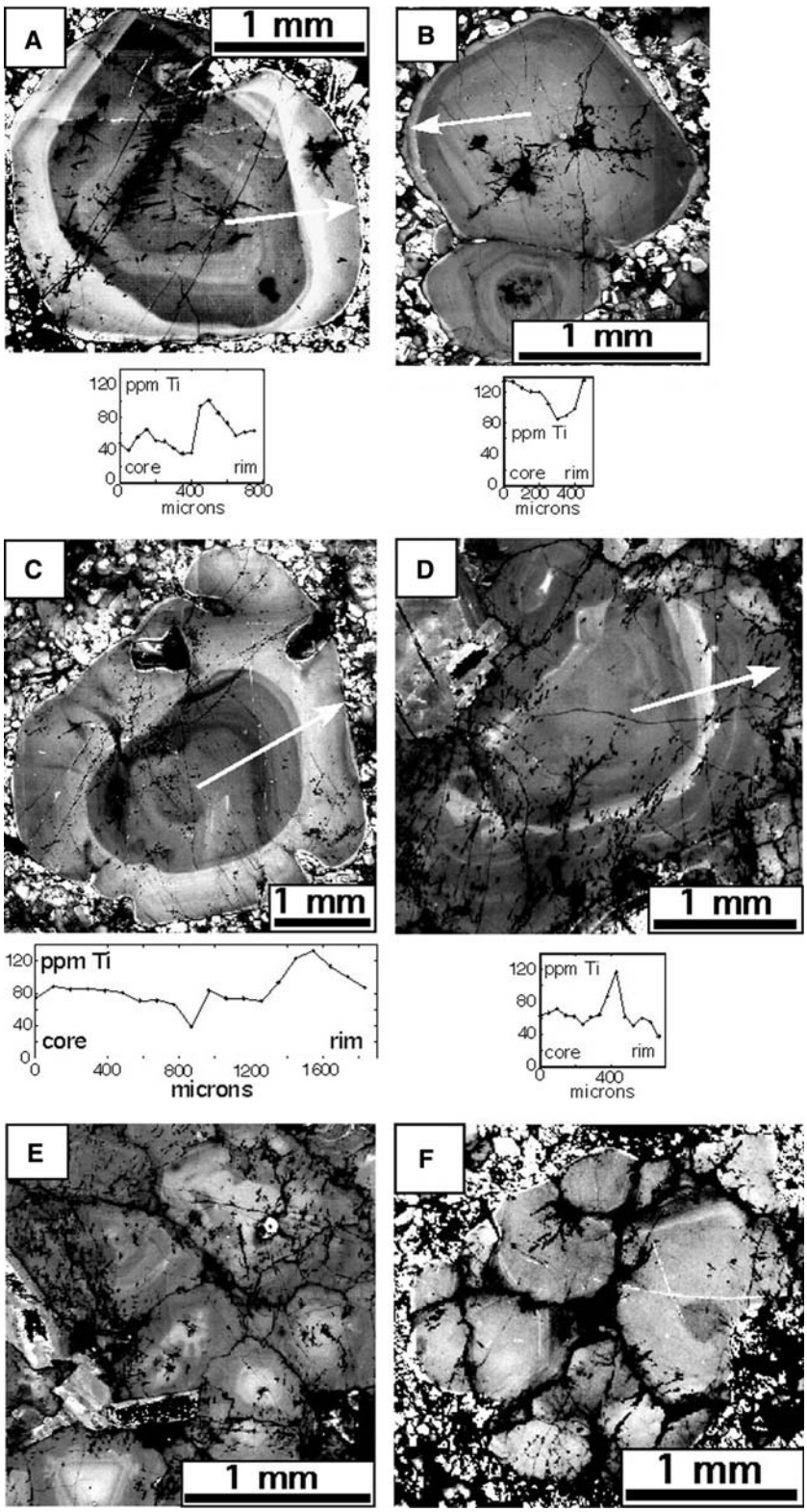

Fig. 6 Characteristic CL and Ti zoning in quartz in intrusive porphyry bodies. **a** Spec. MRM-53. **b** and **c** Spec. MRM-46—(Vinal Cove porphyry). **d**, **e** Spec. MRM-67—(Vinal Cove porphyry). **f** Spec. MRM-53. See Fig. 1 for samples locations

different concentrically zoned centers with truncated margins surrounded by a continuous 15–20 μm thick bright zone; in crossed polars, three distinct optical orientations are apparent.

Felsic enclaves in coarse-grained granite

Quartz crystals in felsic enclaves have complexly zoned cores and ranges of Ti contents comparable to quartz in

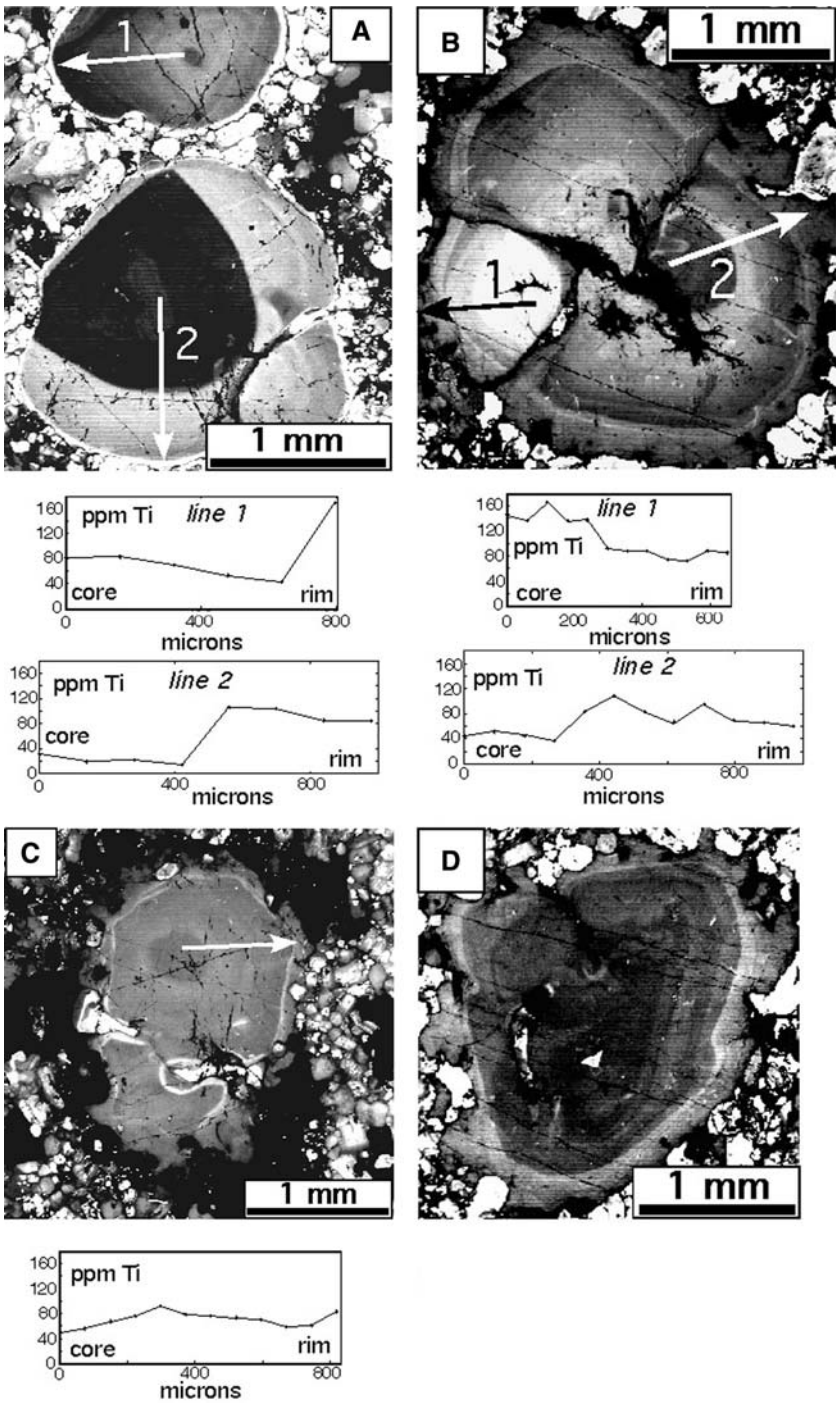

Fig. 7 Characteristic CL and TI zoning in quartz in felsic enclaves in cg granite. **a** Spec. MRM-44D. **b** Spec. WI-34B. **c** Spec. MRM-44D. **d** Spec. WI-34B

both cg granite and in the porphyry (Fig. 7). Where distinct dark cores are visible in CL, they have Ti contents of 20–50 ppm, similar to the range in dark cores of the cg granite and porphyry (Fig. 7a, line 2 and Fig. 7b, line 2). Some enclaves have quartz phenocrysts with a thin outermost bright zone that sharply cuts across zoning in the interior, a feature that is characteristic of quartz crystals in porphyry. Ti contents of these outermost zones are typically above 100 ppm (Fig. 7a, line 1). Some quartz crystals are enclosed within mafic reaction rims (hornblende and biotite). The one example illustrated here (Fig. 7c) shows a thin bright zone just inside the mafic rim; a separate short detailed profile across this bright zone (not shown) indicates that it has an exceptionally high Ti content of 150 ppm. One small (~50 μm) rounded augite crystal occurs within this bright zone.

In other enclaves, quartz crystals may lack the thin bright rim and instead have normally zoned mantles

(Fig. 7b, d). Within any single enclave, these outer zones appear to have consistent widths on all crystals. In contrast, zoning in cores enclosed within the mantle may be highly variable. In apparently synneutic crystals, different members may have cores that contrast greatly in zonal sequence, CL brightness, and Ti concentration (Fig. 7b).

Temperatures of quartz crystallization

The TitaniQ (Ti in quartz) thermometer (Wark and Watson 2006) provides an opportunity to determine the thermal history of quartz crystallization of Vinalhaven felsic rocks from profiles of Ti concentration across the quartz CL zoning. According to the TitaniQ thermometer, the temperature of quartz equilibration can be determined from its Ti content in ppm (C_{Ti}) according to

$$T(\mathrm{K}) = -3,765/[\log\ (C_{Ti}/a_{TiO_2}) - 5.69]$$

where a_{TiO_2} is the activity of TiO_2 relative to that required for rutile saturation (where $a_{TiO_2} = 1$), assuming Henrian behavior. Of course, rutile is rarely, if ever part of the equilibrium assemblage in most granites, and consequently, Ti activity is typically below one. Activity values lower than 0.5 are probably rare in most silicic magmas, however, because a Ti-essential phase such as ilmenite or sphene is generally present (see discussion of Watson et al. 2006). For systems in which Ti activity cannot be precisely determined, the thermometer still yields a minimum temperature of crystallization if used assuming $a_{TiO_2} = 1$ in the equation above. Additionally, relative temperatures—in different zones of an individual crystal, for example can be precisely determined even for systems in which a_{TiO_2} is not constrained, if it can be safely assumed that Ti activity was relatively well buffered by a low-variance mineral assemblage including a Ti-essential phase (such as ilmenite or sphene), if that mineral assemblage did not change during quartz crystallization.

To date, the only igneous system to which the TitaniQ thermometer has been rigorously applied is that which produced the 0.76 Ma, rhyolitic Bishop Tuff (Wark et al. 2007), which has a mineral assemblage (quartz, biotite, magnetite and ilmenite along with both feldspars and zircon) nearly identical to that of the Vinalhaven granites (although with additional, minor pyroxene in some Bishop magmas), and similar bulk-rock compositions as well. There, a_{TiO_2} values calculated from the compositions of coexisting Fe–Ti oxides average ~0.63 (±0.03) for the entire eruption package (Wark et al. 2007), despite a range in eruption temperatures of almost 100°C. Both textural criteria and geochemical variations suggest that Fe–Ti oxides and biotite were crystallizing throughout the solidification of the Vinalhaven granitic magma, and, hence, a comparable a_{TiO_2} should be expected. In addition, by setting a_{TiO_2} to 0.6, TitaniQ temperatures from Vinalhaven quartz rims closely approximate the temperature at the 1 kbar minimum for water-saturated granite. Based on these similarities, we tentatively assign a value of 0.6 to Ti activity (the same value calculated by Wark et al. from coexisting oxides for Bishop magmas) to estimate temperatures of crystallization using the equation above. As discussed by Wark and Watson (2006), if the actual a_{TiO_2} value for Vinalhaven is higher or lower by, for example, 0.1, our temperature estimates will be low or high, respectively, by about 20°C.

Fine-grained granite

Ti concentrations in quartz from fg granite, including dikes, suggest crystallization temperatures in the range 700–770°C, with small cores that may have crystallized at temperatures as high as about 810°C. Based on the Ti zoning, quartz largely crystallized with declining temperatures from core to rim with only minor upward fluctuations in temperature (Fig. 4).

Coarse-grained granite

Overall, quartz in cg granite is complexly zoned with Ti concentrations between 40 and 120 ppm, indicating a range of crystallization temperatures from about 700 to 840°C, assuming that a_{TiO_2} remained constant at 0.6. Outer zones commonly truncate inner zones (consistent with partial quartz resorption) with Ti concentrations increasing sharply (typically by as much as 20–60 ppm, but in some cases by 100 ppm) across the separating boundaries (Fig. 5c, e). If the Ti activity were unchanged at 0.6, those increases in Ti suggest temperature increases in the range of 45–110°C, and uncommonly as much as 150°C, and would still be large even if a_{TiO_2} had increased. These temperature increases are consistent with the heating expected by nearby injection of hot, basaltic magmas preserved as chilled gabbroic bodies within granite. Quartz crystals commonly show multiple zones with abrupt increases in Ti concentration that truncate inner zones, indicating that quartz crystals were affected by multiple episodes of resorption and temperature increase. The high Ti concentrations at the inner margin of each zone decrease gradually toward the rim, consistent with gradually declining temperature after each resorption event.

Ti concentrations are commonly as low as 20 ppm in many small cores of quartz, implying a temperature of only 630–650°C. Because these cores have delicate oscillatory zoning, they appear to be magmatic. One possible explanation is that the cores crystallized at greater depth in the crust and at high a_{H_2O}.

Quartz rims typically have a Ti concentration of about 40 ppm, suggesting a near solidus temperature of about 700°C. Assuming the last existing melt was on the granite minimum and saturated in H_2O, this temperature suggests that final crystallization occurred at a pressure close to 1 kb (Fig. 3), consistent with conditions indicated by metamorphism of country rock blocks (Porter et al. 1999).

Felsic porphyry and enclaves

Quartz crystals in porphyry and in felsic enclaves have cores that closely match Ti concentrations and zoning sequences in the cg granite. Unlike the granite, though, both porphyry and enclaves commonly have a thin rim with Ti concentrations between 120 and 140 ppm with little or no overgrowth of quartz with lower Ti (Figs. 6, 7). The Ti concentrations of these rims indicate temperatures of between about 840 and 860°C. Quartz crystals in those samples with very fine-grained matrix (Figs. 6a–c, f and 7a) typically lack normally zoned margins, suggesting that they quenched immediately after reaching those high temperatures. In samples with a coarser matrix, quartz crystals commonly have lower Ti overgrowths enclosing a thin high Ti zone (Figs. 6d and 7b–d).

Ti-rich zones in quartz crystals that occur within mafic rims (Fig. 7c) may be a case of local disequilibrium, wherein the quartz crystal is dissolving while the mafic phases are growing around it from a melt experiencing diffusive exchange with the bulk magma. The tiny bit of quartz crystallization may have taken place from this ''odd'' melt at the moment of quenching; hence, its very high Ti content. If true, application of the Ti in quartz thermometer here may not be valid.

Regrowth of quartz at higher temperature after resorption

Regrowth of quartz at much higher temperatures after resorption (in cg granite, porphyry and enclaves) requires explanation. The input of substantial volumes of basaltic magma into existing silicic magma chambers must have caused significant thermal perturbations within overlying silicic magma. There is no evidence, however, that mixing of magmas produced melts of intermediate composition within the main body of granite. There is, for example, no strongly reversed zoning in plagioclase, producing An-rich zones. Hence, the common truncation of internal CL zoning by later bright-CL (high Ti) zones should record resorption driven by thermal input, possibly aided by convective self-mixing (Couch et al. 2001), rather than by changes in melt composition (or Ti activity).

If the system is near-eutectic and pressure remains constant, quartz will be stable at elevated temperature only if a_{H_2O} is reduced. Different processes may have contributed to reduction of a_{H_2O}. Because thermal input would melt mainly anhydrous crystals, the a_{H_2O} would necessarily decrease below 1. In addition, the emplacement of relatively dry basaltic magma could contribute to reducing a_{H_2O} in two ways: (1) release of CO_2 as a separate vapor phase (bubbles) into which H_2O is partitioned and (2) transfer of water from H_2O-rich silicic melt into H_2O-poor basaltic melt. Evidence of H_2O transfer into the basalt is found extensively in Vinalhaven mafic rocks that have interacted with felsic magma. The margins of mafic bodies that have commingled with felsic magma are consistently rich in hornblende and biotite, whereas the interiors of these bodies (and dikes that have not commingled with felsic magma) are dominated by augite and olivine with only accessory hydrous phases. Although we do not know with certainty the volatile composition of associated basalts, their low-K tholeiitic compositions and origin in a non-arc, extensional setting is more consistent with a CO_2-rich (rather than H_2O-rich) nature. It appears then, that mafic replenishments both heated and dehydrated resident silicic magma, permitting crystallization of quartz at substantially higher temperatures following these recharge events.

Importance of rejuvenation in the development of granitic plutons

The magnitude of temperature reversals shown by the zoning of quartz crystals in cg granite (Fig. 5) matches closely the magnitude of reversals at the rims of quartz crystals in porphyry (Fig. 6), which appear to be rejuvenated crystal-rich granite (Wiebe et al. 2004). It seems likely that the large reversals in these crystals could record episodes of rejuvenation of nearly solid crystal mush—rather than episodes of resorption within a continually active, melt-rich magma chamber. If true, this strongly supports recent suggestions that plutonic bodies that were built over a long time period did not maintain melt-rich magma chambers for much of that time and, instead, magma chambers may have waxed and waned and been, in general, quite small relative to the size of the resulting pluton (e.g., Wiebe and Collins 1998; Miller and Miller 2002; Hildreth 2004). There is, however, no field evidence in the Vinalhaven intrusion that demonstrates the complete absence of a magma chamber at any time during the growth of the pluton.

Evidence for the rate of cooling

The reversals in Ti concentration in quartz crystals from cg granite and porphyry are very steep (tens of ppm increase rimward across a distance of roughly 20 μm), only slightly less steep than the Ti profiles measured in quartz from the Bishop Tuff by Wark et al. (2007). Based on modeling of Ti diffusion in quartz, Wark et al. (2007) estimated that the Bishop quartz resided at magmatic temperatures for no more than a few hundred years after growth of high-Ti, high-temperature rims prior to quenching by eruption. As shown in Fig. 8, a ~20-micron wide diffusion zone would be established in only 150 years at 800°C and in 3000 years at 700°C. From this, we conclude that the Vinalhaven porphyrys likely cooled to near solidus temperatures (~700°C) in no more than a few thousand years after the rejuvenation event documented by the high-T rims on quartz, consistent with the fine-grained nature of the porphyry matrix and the shallow level of intrusion. Rimward increases in Ti concentration are comparably sharp in many coarse-grained granite samples, suggesting that some of the cg granite cooled over similar time scales.

Character of silicic input

Fg granite dikes are likely feeders for late silicic replenishments to Vinalhaven magma chambers. The fg granite

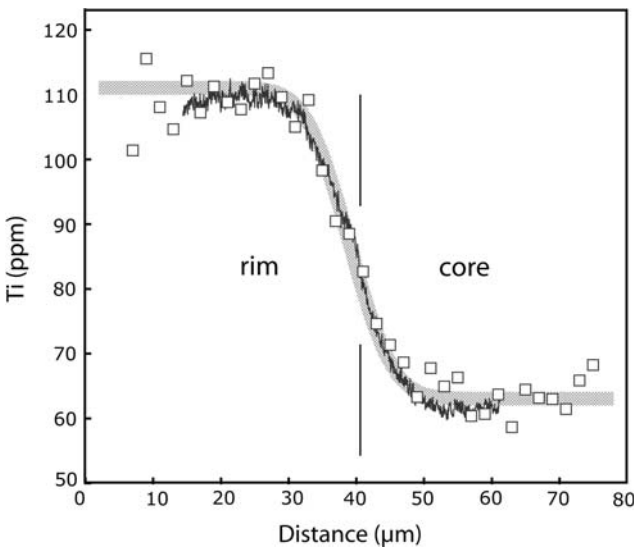

Fig. 8 Plot of Ti concentration (*open squares*) and cathodoluminescence emission intensity (*thin solid line*) across the boundary separating a bright-CL rim from a darker, rounded core in representative quartz in porphyry MRM-46. CL emission intensity was scaled to correspond with measured Ti concentrations on the plot. *Thick shaded line* shows model Ti concentration profile obtained by assuming an initial step-function increase from 62 to110 ppm that was modified by diffusion at 700°C for 3000 years or at 800°C for 150 years, based on Ti diffusivities from Cherniak et al. (2007)

core of the complex appears also to be a replenishment. Because their Sr and Nd isotopic compositions have a strong crustal character and contrast greatly with isotopic compositions of basalts, fg granite could not represent silicic melt that fractionated from basalt. Because fg granite is phenocryst-poor and closely approaches the 1 kb granite minimum (Fig. 3), crystal content was probably low during emplacement. Quartz lacks cores with low Ti concentrations (<40 ppm) that might suggest the crystallization at depth or the presence of restitic metamorphic quartz. However, zircon crystals do commonly have small, inherited cores. The cores of quartz crystals in this granite have Ti concentrations that suggest a maximum temperature of 790–810°C. If, on emplacement, the fg granite was close to 100% melt at 800°C, it should have been undersaturated in H_2O with between 3 and 6 wt.% H_2O (Holtz and Johannes 1994).

Variations in the growth history of quartz in coarse-grained granite

The character of zoning in quartz appears to vary from bottom (early crystallization) to the top (late crystallization) of the granite. Overall, changes in zoning from the basal granites through the mid-level granites to the roof are consistent with known episodes of mafic input. Quartz in samples near the western base of the granite, far from the gabbroic sheets, has a lower range of Ti (100–20 ppm), with rounded cores of 20–40 ppm Ti, fewer and less contrasted reverse zones, and broader, normally zoned rims (Fig. 5d). Quartz crystals from samples within the central area of the granite (north and northwest of the gabbro sheets) (Fig. 1) have the most complex zoning, characteristically with multiple episodes of resorption and corroded cores mantled by high Ti zones. Crystals typically have zones with a wide variation in Ti (140–30 ppm) with increases in Ti as great as 100 ppm in quartz crystallized immediately after resorption. Quartz crystals in samples from near the top (roof) of the granite body have smaller cores with complex zoning but have very broad normally zoned mantles (typically from 100 to 40 ppm Ti) (Fig. 5f). This suggests that, in the later stages of crystallization, quartz grew in a stable environment of gradual cooling, consistent with crystallization from a stagnant magma chamber undisturbed by replenishments.

Quartz zoning in some samples also appears to reflect local thermal events. Quartz crystals from a granite sample within a meter of the Vinal Cove porphyry show minor late resorption and a thin, high Ti rim that could reflect commingling of the granite with the higher temperature porphyry (Fig. 5b). Quartz crystals from a granite sample, immediately below a 5-meter thick gabbroic sheet, show a

strong resorption event and broad high Ti mantles (Fig. 5c). The fabric of the granite indicates compaction and loss of hydrous interstitial melt. Heat from the gabbroic layer was likely responsible for partial dissolution of the quartz, and subsequent crystallization would have occurred at higher temperatures from a relatively H_2O-poor interstitial melt.

Origin of felsic porphyry and enclaves

Field relations, petrography, and feldspar chemistry indicate that porphyry in the Vinal Cove complex formed largely by remelting crystal-rich granitic mush when a large basaltic dike intruded through it (Wiebe et al. 2004). The quartz zoning in these rocks, especially where the sample was in close proximity to the basalt, records a late resorption event followed by growth of high temperature (high Ti) rims and rapid quenching of the porphyry matrix. Remelting of crystal-rich mush would have produced a magma with strongly corroded crystals that was hotter (up to 800–850°C), more melt-rich, and lower in a_{H_2O}. This rejuvenated magma mingled with cooler crystal-rich mush around the margins of the porphyry body. The porphyry matrix appears to have quenched due to its lower a_{H_2O} and hence higher solidus T, because cooling of the porphyry occurred faster than H_2O could diffuse into the rejuvenated, drier porphyry magma. All other bodies of porphyry have comparable quartz zoning and other petrographic characteristics, such as corroded feldspars and disseminated small quenched mafic enclaves, suggesting that all porphyry formed by rejuvenation of crystal-rich granitic mushes.

Felsic enclaves in cg granite have quench textures and quartz crystals with zoning that closely match the porphyry. Similarly, they typically contain small quenched mafic inclusions. In addition, their bulk chemical compositions overlap both with porphyry and cg granite; their trend to lower SiO_2 appears to reflect mechanical mixing of small mafic inclusions. It therefore seems most likely that they also represent rejuvenated crystal-rich mush. They commonly are associated with steep schlieren, indicating they sank through granitic crystal mush with a plastic rheology (Wiebe et al. 2007). Along their basal margins, they are commonly molded around larger crystals in cg granite, indicating that they were not solid when they came to rest. The enclaves probably formed from rejuvenated porphyry magmas (with low a_{H_2O}) that intruded into (i.e., replenished) a melt-rich volume within the granite, breaking apart during flow, quenching, and sinking to a crystal-rich base of a magma chamber. Because enclaves appear to be concentrated in isolated areas, each of these areas may represent a discrete event of rejuvenated silicic replenishment into an existing melt-rich magma chamber.

Implications for a cumulate origin of cg granite

In a single sample of cg granite, cores of different quartz crystals generally appear to have different sequences of zones with different compositions and different numbers of resorption events. Although the crystals occur in contact with each other, their cores appear to record highly varied thermal histories. In contrast, the rims of all quartz crystals show very similar concentrations of Ti that decrease outward to similar values at the crystal margin. Comparison of these closely associated crystals suggests that, during early growth of their cores, they must have been in different environments and have been affected by different thermal histories. Their presence now together seems to require accumulation of crystals, possibly by gravitational settling onto a chamber floor. Crystal accumulation is consistent with the scarce but widespread occurrence of gently dipping layers and schlieren within the granite as well as interlayered chilled mafic sheets in the lower half of the complex (Fig. 1).

Synneusis of quartz crystals, which appears to be widespread and common in cg granite, may also reflect a complex history of crystal accumulation and rejuvenation. In cg granite, equant quartz crystals tend to cluster together between the larger alkali-feldspars. If after deposition these crystals grow substantially from interstitial melt, reducing the porosity to ~10–20%, abundant quartz–quartz contacts will be established. If replenishments of mafic or felsic magma rejuvenate this cumulate, dissolution of quartz (rate-controlled by silica diffusion in the melt) would likely be fastest along cluster margins, rather than along quartz–quartz contacts, resulting in a tendency to preserve clusters of quartz with corroded outer margins. Subsequent crystallization at higher temperatures would produce a continuous Ti-rich quartz rim around multiple cores—a common occurrence in the cg Vinalhaven granite, porphyry, and felsic enclaves.

Conclusions

The thermal record from CL and Ti zoning of quartz in the cg Vinalhaven granite is in accord with field evidence for mafic replenishments into silicic magma chambers. Moreover, quartz in cg granite samples taken from specific locations where thermal histories can be inferred in detail (e.g., beneath a mafic sheet and adjacent to a hotter, drier rejuvenated porphyry) shows zonal sequences that exactly match expectations from field relations. Correlation of quartz zoning with field evidence for a thermal pulse due to mafic input could prove useful for interpreting comparable quartz zoning in erupted rhyolites and in granites that lack direct evidence for mafic input. The more simple zoning of

quartz observed in feeders for silicic replenishments (fg granite) further emphasizes the role of magma chamber processes on the growth histories of crystals in cg granite.

Zoning of CL intensity and Ti content of quartz of cg granite is consistent with multiple resorption events, the larger of which could well represent episodes of rejuvenation of crystal-rich granitic mush. This record of zoning supports recent suggestions that silicic magma chambers wax and wane in response to varied rates and compositions of replenishments though time and place (Mahood 1990; Hildreth 2004). This small intrusive complex appears to have crystallized over a time period of ~1 m.y., and the record of quartz zoning suggests that pluton growth occurred with brief episodes of replenishment and rejuvenation interrupting long periods of cooling and crystallization.

Acknowledgments Funding was provided in part by NSF awards EAR-0536655 to RAW, EAR-0409622 to DAW and EAR-0536969 to DPH and by a Hackman Faculty Research Award to RAW from Franklin and Marshall College.

References

Cherniak DJ, Watson EB, Wark DA (2007) Ti diffusion in quartz. Chem Geol 236:65–74

Couch S, Sparks RSJ, Carroll MR (2001) Mineral disequilibrium in lavas explained by convective self-mixing in open magma chambers. Nature 411:1037–1039

D'Lemos RS, Kearsley AT, Pembroke JW, Watt GR, Wright P (1997) Complex quartz growth histories in granite revealed by scanning cathodoluminescence techniques. Geol Mag 134:549–552

Emeleus CH (1963) Structural and petrographic observations on layered granites from southern Greenland. Min Soc Am Spec Pap 1:22–29

Gilbert GK (1906) Gravitational assemblage in granite. Geol Soc Am Bull 17:321–328

Govindaraju K (1994) 1994 Compilation of working values and sample description for 383 geostandards. Geostandards Newsl 18(Special issue):1–158

Hawkins DP, Wiebe RA (2004) Discrete stoping events in granite plutons: a signature of eruptions from silicic magma chambers? Geology 32:1021–1024

Hildreth W (2004) Volcanological perspectives on long Valley, Mammoth Mountain, and Mono Craters: several contiguous but discrete systems. J Volc Geotherm Res 136:169–198

Hodge DS, Abbey DA, Harbin MA, Patterson JL, Ring MJ, Sweeny JF (1982) Gravity studies of subsurface mass distribution of granitic rock in Maine and New Hampshire. Am J Sci 282:1289–1234

Hogan JP (1993) Monomineralic glomerocrysts: Textural evidence for mineral resorption during crystallization of igneous rocks. J Geol 101:531–540

Hogan JP, Sinha AK (1989) Compositional variation of plutonism in the coastal Maine magmatic province: mode of origin and tectonic setting. In: Tucker RD, Marvinney RG (eds) Studies of maine geology: igneous and metamorphic geology. Maine Geo Surv Dept Cons 4:1–33

Holtz F, Johannes W (1994) Maximum and minimum water contents of granitic melts: implications for chemical and physical properties of ascending magmas. Lithos 32:149–159

Loomis TP, Welber PW (1982) Crystallization processes in the Rocky Hill granodiorite pluton, California: an interpretation based on compositional zoning of plagioclase. Contrib Mineral Petrol 81:230–239

Mahood GA (1990) Second reply to comment of RSJ Sparks, HE Huppert and CJN Wilson on ''Evidence for long residence times of rhyolitic magma in the Long Valley magmatic system: the isotopic record in the precaldera lavas of Glass Mountain''. Earth Planet Sci Lett 99:395–399

Miller CF, Miller JS (2002) Contrasting stratified plutons exposed in tilt blocks, Eldorado Mountains, Colorado River Rift, Nevada, USA. Lithos 61:209–224

Müller A, Breiter K, Seltmann R, Pécskay Z (2005) Quartz and feldspar zoning in the eastern Erzgebirge volcano-plutonic complex (Germany, Czech Republic): evidence of multiple magma mixing. Lithos 80:201–227

Müller A, Seltmann R, Behr H-J (2000) Application of cathodoluminescence to magmatic quartz in a tin granite—case study from the Schellerhay granite complex, eastern Erzgebirge, Germany. Mineralium Deposita 35:169–189

Porter BS, Wiebe RA, Cheney JT (1999) Regional and contact metamorphism of Paleozoic greenschist and pelites, Vinalhaven Island, Maine. Geol Soc Am Abstracts with Programs 31, no. 2:A-61

Robinson DM, Miller CF (1999) Record of magma chamber processes preserved in accessory mineral assemblages, Aztec Wash pluton, Nevada. Am Min 84:1346–1353

Vance JA (1969) On synneusis. Contrib Mineral Petrol 24:7–29

Wallace GS, Bergantz GW (2005) Reconciling heterogeneity in crystal zoning data: an application of shared characteristic diagrams at Chaos Crags, Lassen Volcanic Center, California. Contrib Mineral Petrol 149:98–112

Wark DA, Spear FS (2005) Titanium in quartz: Cathodoluminescence and thermometry. Geochim Cosmochim Acta 69:A592

Wark DA, Watson EB (2006) The TitaniQ: a Titanium-in-Quartz Geothermometer. Contrib Mineral Petrol 152:743–754

Wark DA, Hildreth W, Spear FS, Cherniak DJ, Watson EB (2007) Pre-eruption recharge of the Bishop magma chamber. Geology 35:235–238

Watson EB, Wark DA, Thomas JB (2006) Crystallization thermometers for zircon and rutile. Contrib Mineral Petrol 151:413–433

Wiebe RA (1968) Plagioclase stratigraphy: a record of magmatic conditions and events in a granite stock. Am J Sci 266:690–703

Wiebe RA (1993) The pleasant bay layered gabbro-diorite, coastal maine: ponding and crystallization of basaltic injections into a silicic magma chamber. J Petrol 34:461–489

Wiebe RA, Collins WJ (1998) Depositional features and stratigraphic sections in granitic plutons: implications for the emplacement and crystallization of granitic magma. J Struct Geol 20:1273–1289

Wiebe RA, Hawkins DP (2004) Multiple replenishments in an evolving silicic magma chamber: the Vinalhaven intrusive complex, Maine, USA. Geochim Cosmochim Acta 68(11S):A672

Wiebe RA, Jellinek M, Markley MJ, Hawkins DP, Snyder D (2007) Steep schlieren and associated enclaves in the Vinalhaven granite, maine: possible indicators for granite rheology. Contrib Mineral Petrol 153:121–138

Wiebe RA, Manon MR, Hawkins DP, McDonough WF (2004) Late stage mafic injection and thermal rejuvenation of the Vinalhaven granite, coastal Maine. J Petrol 45:2133–2153